Journal of Engineering Research and Applied Science
Available at www.journaleras.com
Volume 10 (1), June 2021, pp 1703-1716
ISSN 2147-3471 © 2021

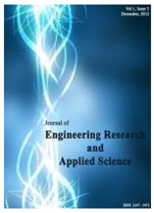

Petrological characteristics of eocene volcanic rocks around Demirören (Gümüşhane, NE Turkey)

A. Vural[1,a], İ. Akpınar[1], A. Kaygusuz[1], F. Sipahi[1]

[1]Gümüşhane University, Geological Engineering, Gümüşhane, Turkey.

Accepted 06 April 2021

Abstract

In this study, the Eocene volcanic rocks that crop out in Demirören (Gümüşhane) and its surroundings in the South Zone of the Eastern Pontides were studied mineralogically, petrographically and geochemically. Eocene aged Demirören volcanics are in basaltic andesite, andesite, dacite and rhyolite in composition and consist mainly of plagioclase, alkali feldspar, quartz, hornblende, augite and biotite minerals. These rocks are calc-alkaline in character and have low to high-K content. They are also enriched in large ion lithophile elements (LILEs) and light rare earth elements (LREEs) and depleted in the high field strength elements (HFSEs). The chondrite-normalized rare earth element distributions are concave-shaped with low to medium enrichment (LaN/LuN = 4-16), indicating that the rocks forming the volcanics originated from the same source. Fractional crystallization and minor assimilation ± magma mixing played a role in the development of the volcanites. All these data indicate that the parental magma of the volcanites could possibly be a source of sub-continental lithospheric mantle, enriched by the metasomatism of fluids previously derived from subduction-related.

Keywords: Eastern pontides, eocene, geochemistry, Demirören volcanics, petrology

1. Introduction

The Eastern Pontides, located in the Alpine-Himalayan orogenic belt and also known as the Sakarya Zone, are one of the regions where volcanic and plutonic rocks are widely observed and important mineral deposits have also developed [1, 2, 11–18, 3–10]. Three main volcanic circuits have been identified in the Eastern Pontides: Liassic, Cretaceous and Eocene (and later) [19, 20]. The Eastern Pontides are divided into two zone by Özsayar [21] as northern and southern zones since Cretaceous rocks are lithologically different in the northern and southern regions. Accordingly, the study area is in the south zone of the Eastern Pontides.

Although the Eocene plutonic rocks in the Eastern Pontides have been geochemically, isotopically and geochronologically well studied [22–26], studies on their volcanic equivalents are limited [27–31].

In the Demirören (Gümüşhane) region, detailed studies have been conducted mainly on general geology, mineral/ore deposits, and also environmental geochemistry; but studies on the petrology of Eocene aged volcanic rocks are limited in this area [17, 32]

In this study, the petrographic, geochemical and petrological characteristics of the Eocene Demirören (Gümüşhane) volcanics were revealed, and the development of Eastern Pontide Tertiary magmatism was tried to be clarified.

2. Regional geology and stratigraphy

The pre-Late Cretaceous rocks are represented by early Carboniferous metamorphic rocks [33], Middle to Late Carboniferous plutonic rocks [34–37], Jurassic volcanics, volcaniclastic and plutonic rocks [38, 39] and Late Jurassic-Early Cretaceous carbonates [40]. The Late Cretaceous series that unconformably overlie carbonate rocks consist of volcanic, plutonic and sedimentary rocks [41–44], and overlain by the Cenozoic units. The Cenozoic units in the region are represented by Late Paleocene-

[a] Corresponding author; alaaddinvural@hotmail.com

Early Eocene adakitic rocks [45, 46], Middle Eocene volcanic, sub-volcanic and sedimentary rocks [10, 11, 50, 12, 27, 30, 31, 39, 47–49], Middle Eocene plutonic rocks [16, 18, 22, 23, 26, 51, 52], Neogene volcanic rocks [53], Late Miocene-Pliocene adakitic volcanic-subvolcanic rocks [54]. While the Miocene and post-Miocene magmatism's were calc-alkaline to alkaline compositions in the Trabzon-Gümüşhane areas [53, 54], they show calc-alkaline composition in the Kandilli-Ilıca areas [55, 56]. The youngest units in the region are Quaternary alluvium and terraces [57].

The study area located in the south zone of the Eastern Pontides and is generally dominated by volcanic and plutonic rocks (Figure 1). The oldest rocks in the study area are represented by Late Cretaceous aged basalt-andesite lava and pyroclastics rocks. These rocks are overlain conformably by Late Cretaceous aged limestones. Eocene aged volcanics and volcano-clastic rocks (Kabaköy Formation) unconformably overlies these units. Eocene rocks start with the basal conglomerate at the bottom and transition to andesite, basalts and their pyroclastics (Kabaköy Formation) upwards. All these units were cut by the Middle-Late Eocene granodiorites-quartz porphyries (Figure 1).

3. Analysis Methods

Within the scope of the study, thin sections of rock samples collected from the field were prepared and detailed petrographic properties were determined under polarizing microscope. Major, trace and rare earth element analyzes of 8 rock samples belonging to the study area were carried out in Vancouver, BC Analysis Laboratory (ACME) in Canada. Major and trace elements were analyzed by ICP (Inductively Coupled Plasma) method, and rare earth elements (REE) by ICP-MS (Inductively Coupled Plasma – Mass Spectrometry) method. For the major and trace element analyzes, 0.2 grams of powder sample was mixed with 1.5 grams of $LiBO_2$ and analyzed after dissolving in a liquid containing 5% HNO_3, while 0.250 grams of powder sample for rare earth element analyzes was dissolved in four different acids and analyzed. Loss on ignition (LOI) ratios of the samples were calculated from the weight difference by heating the samples at 1000 °C. Total Fe content is expressed in terms of Fe_2O_3. Detection limits range from 0.002 to 0.04 wt% for major oxides, 0.1 to 8 ppm for trace elements, and 0.01 to 0.3 ppm for REE.

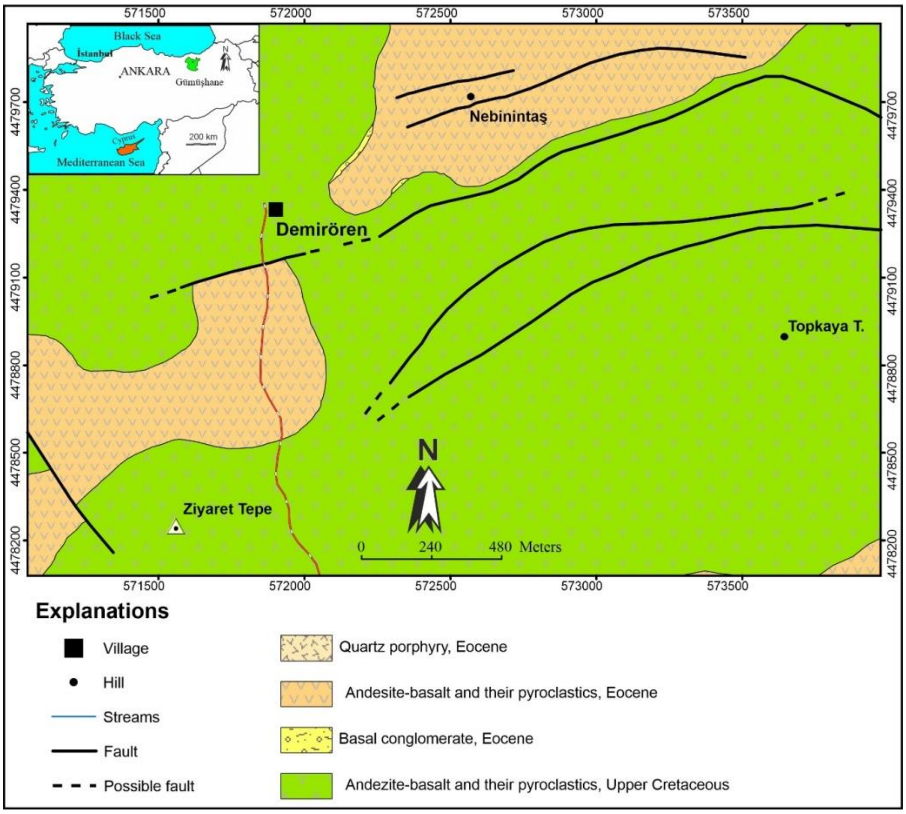

Figure 1. Geological map of the study area (after [3])

4. Mineralogy and petrography

According to their petrographic and textural features, the studied volcanic rocks consist of basaltic andesites, andesites, dacites and rhyolites (Figure 2).

Basaltic andesites and andesites have porphyritic, microlithic porphyritic and glomerophyric textures (Figure 2). Major minerals consist of plagioclase, pyroxene, hornblende, biotite and opaque minerals. Plagioclases are found as coarse, euhedral and semi-euhedral elongated crystals and small crystals in the groundmass. Coarse crystals generally show a zoned texture. In some minerals, albite twin and polysynthetic twins are seen. The most common alteration products are calcite, chlorite and clay minerals. Hornblendes are seen as coarse, euhedral and semi-euhedral prismatic crystals and small crystals in the groundmass. Some minerals contain plagioclase and opaque mineral inclusions. Generally, it has been dissociated into calcite and opaque minerals developed in the margins. Pyroxenes are generally seen as coarse prismatic crystals and small grains in some sections in the groundmass. Biotites are generally in the form of small prismatic crystals and are seen in some sections. Reddish brown and yellowish brown pleochroism is evident. Opaque minerals are scattered with a small grain. Secondary minerals are composed of calcite, chlorite, sericite and epidote minerals. Secondary quartz veins are also observed in some samples. The groundmass consists of micro and crypto crystals plagioclase, augite, hornblende and biotite minerals and opaque mineral grains (Figure 2).

Dacites/rhyolites have microgranular, porphyritic and partially hyalo-porphyritic in texture (Figure 2). Major minerals consist of plagioclase, hornblende, biotite and opaque minerals. Plagioclases are found as coarse, euhedral lath-shaped crystals and microliths in groundmass. Plagioclases show albite and albite-carlsbad twins in order of abundance. In some samples, zoned plagioclase crystals are seen. The most common alteration types are sericitization, calcification and clay formations. Quartz is generally form of euhedral crystals. Coarse crystals generally show undulated extinction and are fractured. Biotites are in the form of euhedral and subhedral prismatic crystals and lamellar. In some sections, they are observed as being partially decomposed from the edges and converted to chlorite. Hornblendes are in the form of euhedral and subhedral plate-like prismatic crystals. In some sections, it is seen as decomposed into chlorite and calcite. Opaque minerals exist as euhedral and subhedral crystals, both coarse and small. The groundmass consists of micro and crypto-crystals of plagioclase, quartz, biotite, hornblende and opaque minerals. Secondary minerals are composed of zircon and apatite minerals. Secondary quartz minerals were observed in some samples. The alteration minerals are chlorite, sericite and calcite.

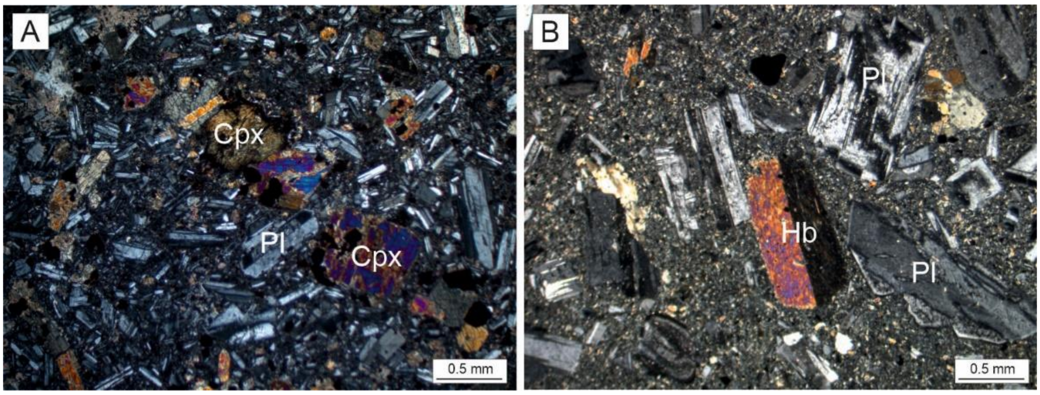

Figure 2. Demirören volcanics, a) Microlithic porphyritic texture in basaltic andesites, b) Porphyritic texture in andesites (Crossed Polar, Pl: Plagioclase, Hb: Hornblende, Cpx: Clino-pyroxene)

5. Geochemical features of Eocene Demirören volcanics

5.1. Major and trace elements

Major, trace and rare earth element analyzes of eight samples belonging to Demirören volcanics are given in Table 1.

SiO_2 values of the studied samples are between 52 and 77%, the lowest in basaltic andesites (52-53) and the highest in rhyolites (73-77). The K_2O/Na_2O ratios of the samples vary between 0.1-20.5 and the magnesium numbers [Mg # = 100 * (MgO / MgO + $Fe_2O_3^T$)] between 35 and 69 (Table 1).

On the SiO_2 versus (Na_2O+K_2O) diagram [58], Demirören volcanics consist of subalkaline basaltic andesite, andesite, dacite and rhyolite in composition (Figure 3a). In [59]'s SiO_2-Zr/TiO_2 diagram, it is seen that the samples are generally composed of basalt, andesite, dacite and rhyolite in composition (Figure 3b).

Table 1. Major (%), trace and rare earth element (ppm) analyzes of the samples of Demirören volcanics.

Rock	**Basaltic andesite**		**Andesite**			**Dacite**	**Rhyolite**	
Sample	Duy-1	Duy-2	EOB-2	EOB-4	Ak-3	NÇ-137	TA-3	TA-5
SiO_2	51.48	52.63	59.04	60.59	61.28	71.15	73.03	76.58
TiO_2	1.17	0.83	0.73	0.59	0.66	0.38	0.16	0.11
Al_2O_3	16.87	18.17	16.27	15.97	15.48	15.79	12.89	12.22
Fe_2O_3	8.69	9.11	7.14	6.37	6.13	3.26	2.88	1.08
MnO	0.11	0.11	0.13	0.12	0.11	0.01	0.33	0.04
MgO	3.78	6.88	3.20	3.44	2.24	0.41	0.69	1.10
CaO	8.59	1.02	6.06	5.08	5.06	0.02	0.79	0.15
Na_2O	2.65	0.63	2.95	3.25	2.81	0.23	2.40	2.22
K_2O	0.27	2.96	2.25	1.77	1.87	4.71	2.83	4.16
P_2O_5	0.23	0.11	0.16	0.13	0.16	0.07	0.06	0.04
LOI	5.90	7.30	1.80	2.50	4.00	1.90	3.80	2.10
Total	99.75	99.78	99.76	99.78	99.81	99.90	99.85	99.83
Co	20.80	22.80	16.70	16.30	13.20	0.20	4.80	1.00
Ni	3.40	9.10	7.60	8.70	5.10	1.10	6.30	2.20
V	262.00	219.00	178.00	156.00	136.00	33.00	30.00	14.00
Cu	27.20	18.50	58.40	36.20	40.80	83.60	17.60	2.00
Pb	8.10	6.40	7.30	3.90	6.70	9.30	42.90	24.10
Zn	78.00	114.00	29.00	42.00	36.00	3.00	160.00	21.00
W	0.50	4.80	0.90	0.80	0.70	6.60	0.50	0.50
Rb	4.60	78.20	54.20	38.90	50.70	120.10	103.10	114.70
Ba	432.00	271.00	608.00	576.00	501.00	298.00	812.00	1151.00
Sr	454.30	66.80	339.40	305.50	286.10	7.90	72.10	78.70
Ta	0.30	0.30	0.40	0.50	0.20	0.70	0.60	0.70
Nb	6.80	5.70	7.10	6.50	5.90	12.70	8.70	8.10
Hf	2.80	2.70	4.20	3.40	3.60	6.80	2.30	2.10
Zr	107.40	105.30	142.60	119.80	131.70	209.40	75.20	64.70
Y	21.70	20.50	21.10	19.10	22.20	26.60	10.30	5.80
Th	2.90	1.90	6.40	6.30	5.90	10.60	13.10	11.20
U	0.60	0.80	1.60	1.40	1.40	1.50	3.50	3.30
Ga	19.10	20.20	16.10	15.60	13.10	20.40	14.70	12.30
La	17.30	13.60	20.50	20.30	21.20	26.60	26.10	24.50
Ce	32.40	22.40	37.30	36.90	38.20	48.40	39.10	35.90
Pr	4.34	3.31	4.99	4.64	4.98	6.09	4.01	3.69
Nd	17.80	12.90	19.00	16.80	20.10	20.90	12.80	11.40
Sm	3.71	3.08	4.01	3.42	4.21	3.88	1.97	1.55
Eu	1.24	0.69	0.93	0.84	1.02	0.56	0.44	0.35
Gd	3.99	3.30	4.08	3.52	4.09	4.02	1.65	1.19
Tb	0.60	0.51	0.64	0.58	0.65	0.76	0.25	0.17
Dy	3.94	3.14	3.83	3.50	4.10	4.57	1.47	1.01
Ho	0.73	0.67	0.80	0.76	0.87	0.98	0.35	0.20
Er	2.21	2.17	2.47	2.09	2.45	2.90	1.13	0.72
Tm	0.33	0.32	0.37	0.34	0.35	0.41	0.17	0.12
Yb	2.04	2.21	2.32	2.20	2.27	2.96	1.26	0.91
Lu	0.34	0.40	0.38	0.35	0.38	0.44	0.20	0.16
$(Eu/Eu^*)_n$	0.98	0.66	0.70	0.73	0.74	0.43	0.73	0.76
$(La/Lu)_n$	5.27	3.52	5.59	6.01	5.78	6.26	13.51	15.85
Mg #	48.92	62.44	49.66	54.31	44.58	21.68	34.53	69.16
K_2O/Na_2O	0.10	4.70	0.76	0.54	0.67	20.48	1.18	1.87

Nb/La	0.39	0.42	0.35	0.32	0.28	0.48	0.33	0.33
Ba/Nb	63.53	47.54	85.63	88.62	84.92	23.46	93.33	142.10
La/Nb	2.54	2.39	2.89	3.12	3.59	2.09	3.00	3.02
Ce/Pb	4.00	3.50	5.11	9.46	5.70	5.20	0.91	1.49

Mg# (mg-number) = molar 100xMgO/(MgO+ $Fe_2O_3^T$), LOI is loss on ignition, Eu*=$(Sm+Gd)_{cn}/2$

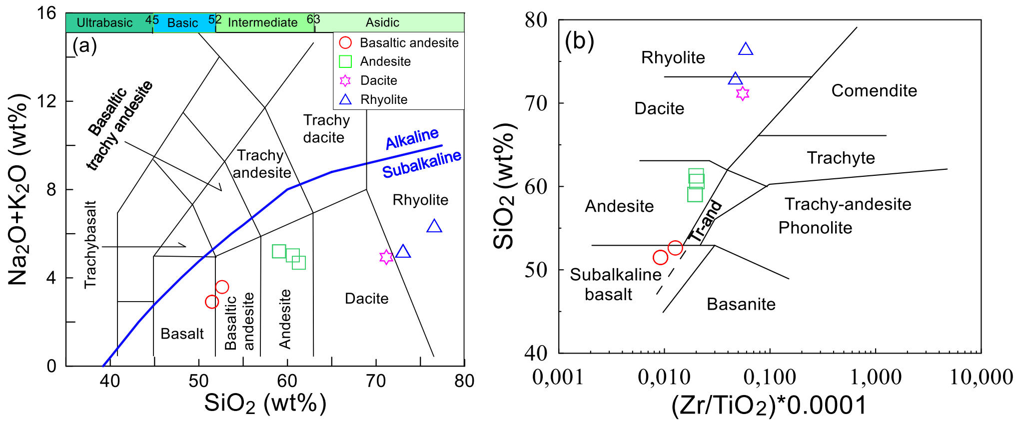

Figure 3. Demirören volcanics' a) SiO_2 versus total alkali (Na_2O+K_2O) diagram [58] b) Zr/TiO_2 against SiO_2 classification diagram [59] (Alkali / subalkaline separation curve is taken from [60])

All samples in the AFM diagram are calc-alkaline in characters (Figure 4a). When the rock samples are plotted to the K_2O-SiO_2 diagram [58], it is seen that the samples have low to high-K content (Figure 4b).

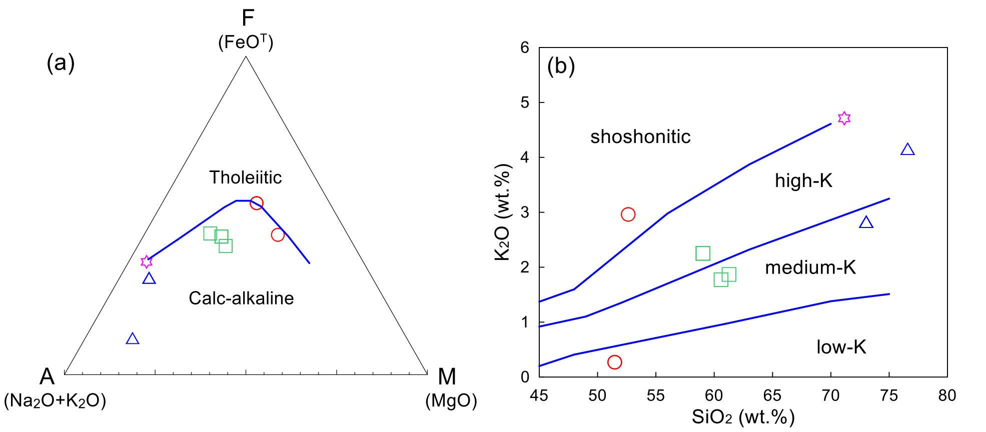

Figure 4. Demirören volcanics' a) AFM diagram (tholeiitic-calc alkaline separation curve taken from [60]), b) SiO_2 versus K_2O diagram (The field boundaries between medium-K, high-K and shoshonitic are from [61]).

Although irregular distributions are observed in Na_2O (Figures 5 and 6), the other samples have a good correlation between SiO_2 vs. major and trace elements indicated that fractional crystallization plays an important role in the development of the Demirören volcanic rocks. In Harker diagrams, CaO, MgO, Al_2O_3, $Fe_2O_3^T$, P_2O_5 and TiO_2 decrease with increasing silica (Figure 5). A positive correlation is also observed in K_2O vs. SiO_2 (Figure 5).

In trace element variation diagrams, a positive correlation is observed in Pb, Ba, Rb, Nb and Th values, and a negative relationship is observed in Sr, Y and Ni values with increasing SiO_2 (Figure 6).

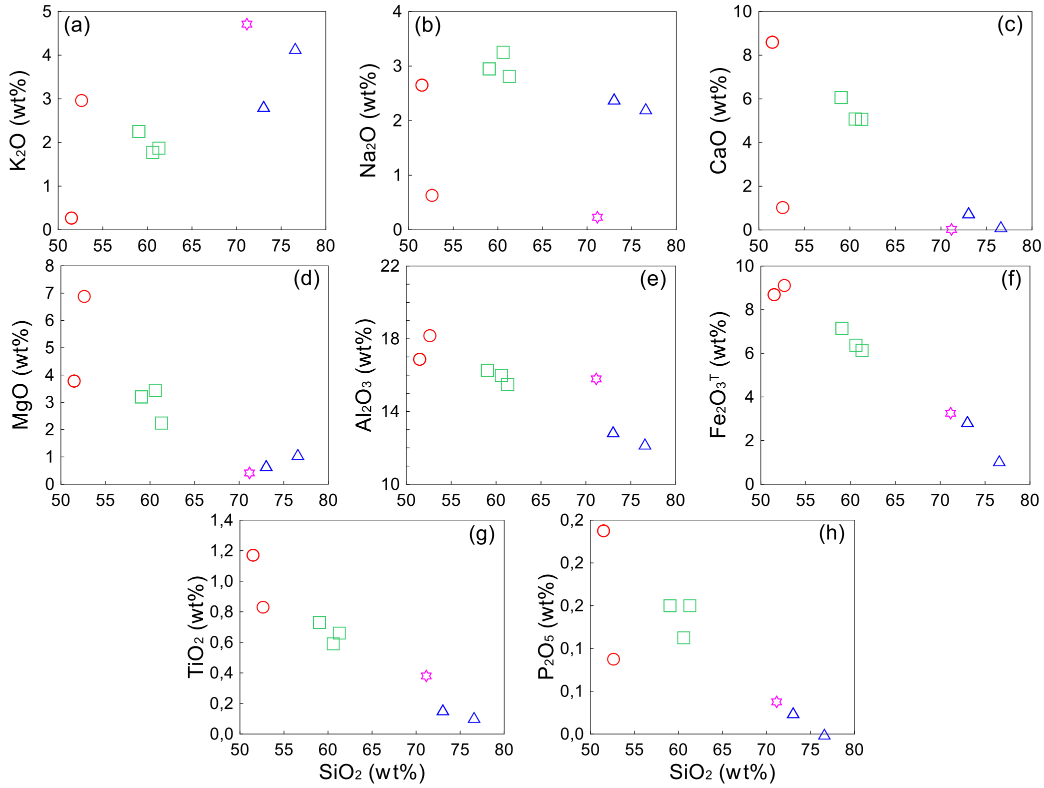

Figure 5. Major element variation diagrams of the Demirören volcanics rock

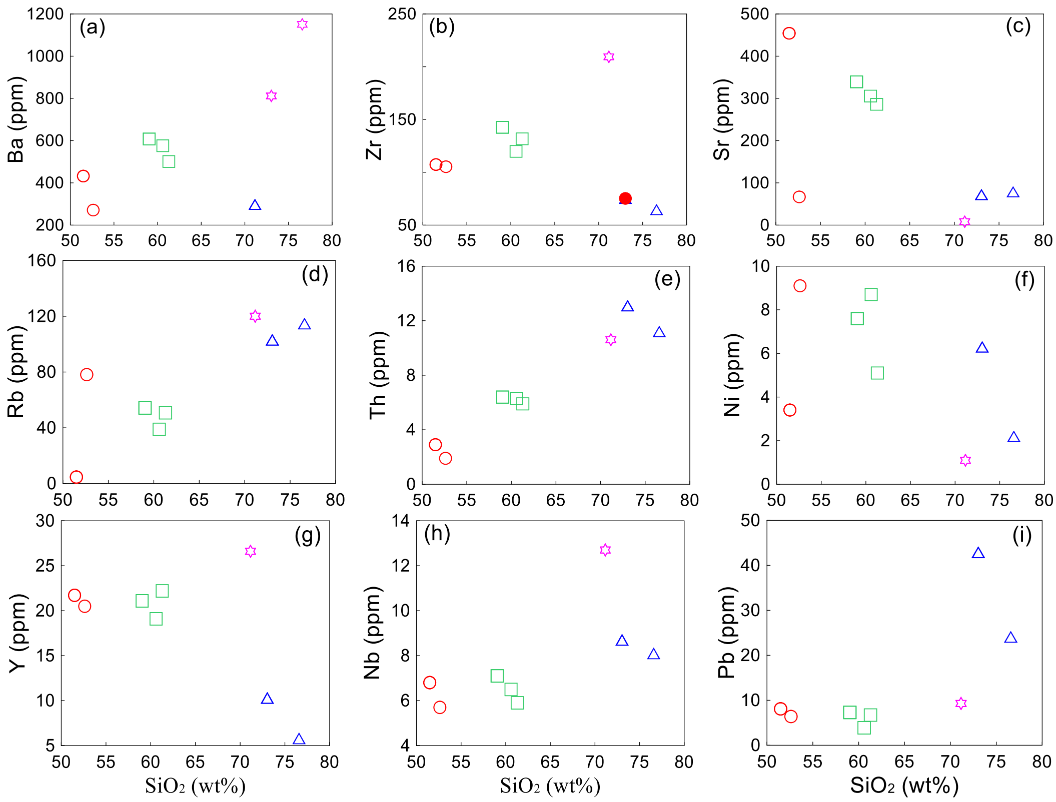

Figure **6.** Trace element variation diagrams of the Demirören volcanics rock

In primitive mantle-normalized [62] spider diagrams, while the samples exhibit enrichment in large ion lithophile elements (LILEs), the depletion is observed in terms of compatible elements such as Ti, Nb and Ta (Figure 7). The negative Nb and Ta anomalies show that the subduction component plays an active role in the development of the main magma of the rocks.

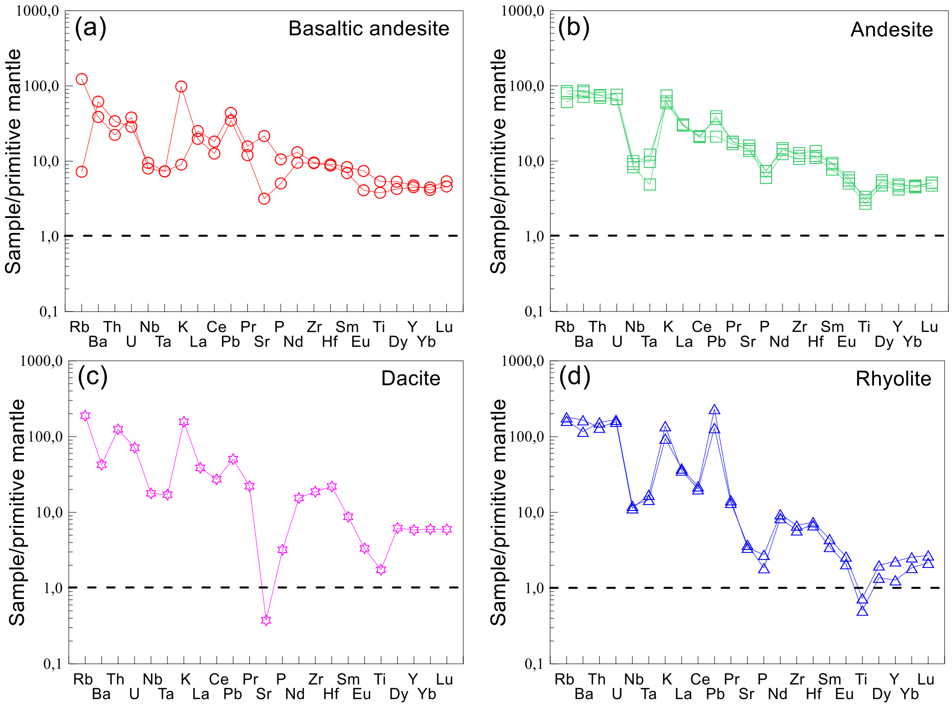

Figure 7. Trace element distribution diagrams of Demirören volcanics (Normalized values after [62]

Chondrite-normalized (Taylor and McLennan 1985) rare earth element distributions of the studied volcanic rocks are shown in Figure 8. All of the samples has parallel patterns to each other, this indicates that all of the rocks of the volcanics are derived from a similar mantle source. Light rare earth elements (LILEs) are enriched more than heavy rare earth elements (HREEs) (Figure 8). The $(La/Lu)_N$ ratios of the samples range from 3.5 to 15.9 (Table 1). Negative Eu anomalies (Eu/Eu* = 0.43-0.98) is observed in all of the samples (Figure 8; Table 1).

The tectonic environments of the studied volcanics were tried to be determined according to the relationship of elements such as Ti, Zr, Sr and Nb, which are known not to be affected by alteration. According to the Nb versus Nb/Th tectonic discrimination diagram [63], the samples fall into the area of arc volcanics and nearby places (Figure 9a). In the Sr / Y versus Y discrimination diagram (Drummond and Defant, 1990), the samples are located in the area of the normal arc volcanic series (Figure 9b).

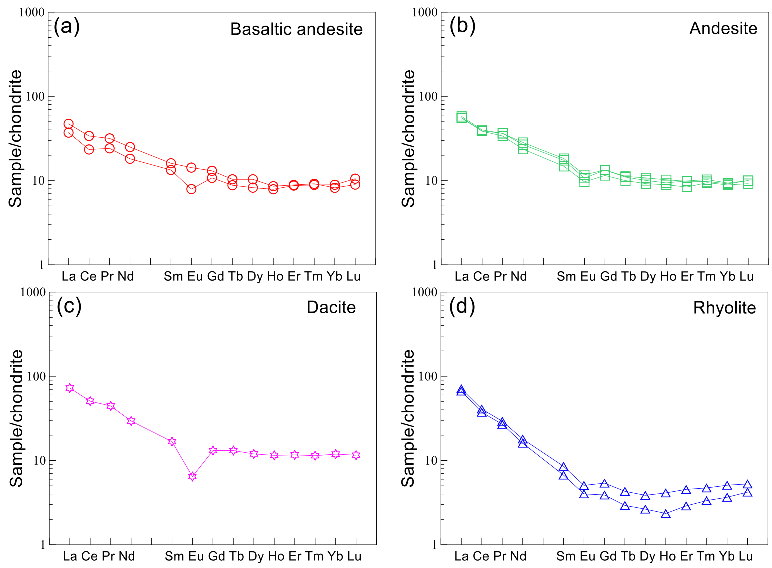

Figure 8. Rare earth element distributions of the Demirören volcanics rocks (Normalized values after [64]

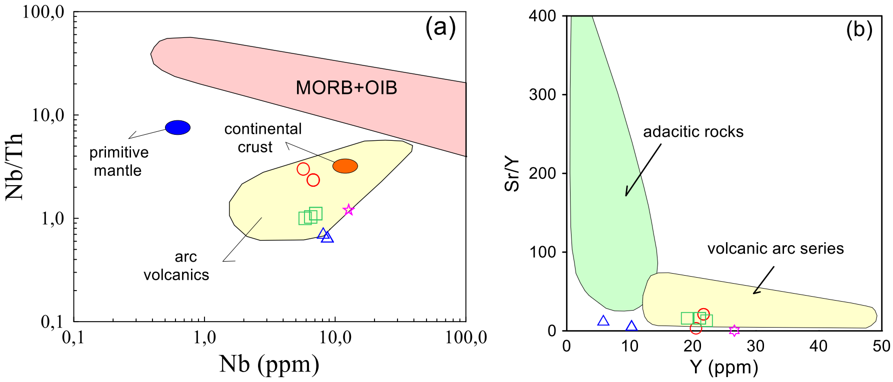

Figure 9. Tectonic discrimination diagrams of the Demirören volcanics. a) Nb (ppm) versus Nb / Th diagram (The primary mantle values are taken from [65], continental basalt, MORB, OIB and arc volcanic values from [66]) b) Sr / Y versus Y diagram [67]

6. Discussion

Considering whole rock major, trace and rare earth data (Figures 5 and 6; Table 1), it is seen that clinopyroxene, plagioclase, hornblende and Fe-Ti oxide fractionation is important in the development of the studied volcanic rocks. The gradual decrease in TiO_2 and $Fe_2O_3^T$ contents with the increasing SiO_2 content indicates the fractionation of Fe-Ti oxides. The negative relationships in CaO, $Fe_2O_3^T$ and MgO against SiO_2 indicate that plagioclase (An> 50) and clinopyroxene phases are fractionation from the main magma (Figure 5). The negative correlation of SiO_2 against $Fe_2O_3^T$ and Al_2O_3 indicates hornblende fractionation. Scattering is observed in the SiO_2 versus Na_2O diagram, this indicates that alteration events are partially effective. There are positive relationships against SiO_2 against K_2O diagram, indicates the fractionation of basic plagioclase. The negative correlation observed in the P_2O_5 vs. SiO_2 reflects the apatite fractionation. Ni reduction against SiO_2 supports the clinopyroxene fractionation (Figure 6). In the Y versus CaO diagram (Figure 10a), the studied samples show a J-type trend, expressing that hornblende and clinopyroxene fractionation is effective. The trend observed in Ba/Sr versus Sr diagram (Figure 10b) show plagioclase fractionation.

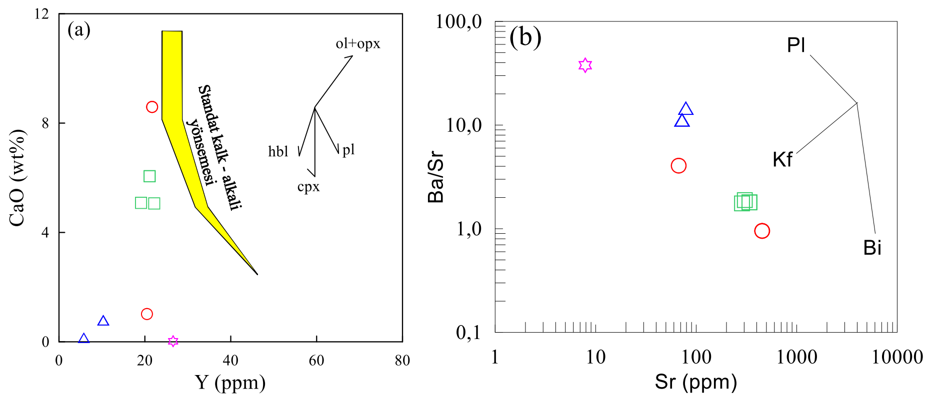

Figure 10. Y (ppm) versus CaO (%) diagram of Demirören volcanics [68], Vectors show the fractionation directions of minerals for basaltic composition.

Negative trends observed in Y / Nb ratios against SiO_2 diagram indicate crustal assimilation during magma development (Figure 11a). Th / Yb and Ta / Yb ratios are used effectively in determination of source composition and crustal contamination. This is due to the fact that the Th element is affected more than Ta and Yb in crustal contamination [69]. In the Th / Yb versus Ta / Yb diagram (Figure 11b), the studied volcanic rocks form a trend sub-parallel to the mantle array but shifted to higher Th/Yb ratios. This suggests melt derivation from a source, which had been previously enriched (or metasomatized) by fluids derived from an earlier (i.e., pre-Eocene) subduction processes.

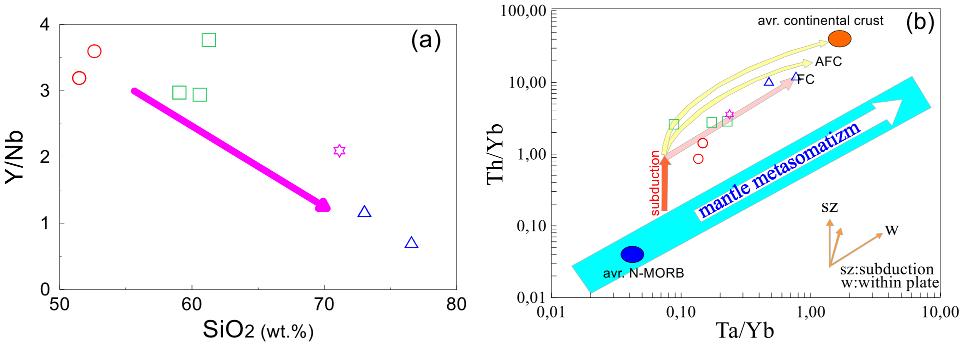

Figure 11. Demirören volcanics' a) SiO_2 versus Y/Nb diagram, b) Ta/Yb versus Th/Yb diagram [69] (Vectors showing subduction enrichment and mantle metasomatism are taken from [69], N-type MORB and average upper crust values are taken from [64, 70])

The enrichment of LILE elements (K, Sr, Rb and Ba), Th and Ce, and high Th / Yb ratios observed in Demirören volcanic rocks indicate that the main magma of the volcanites may have been derived from the lithospheric mantle source [71, 72]. In addition, Nb and Ta depletion compared to LILE elements observed in the studied volcanic rocks expresses the property of the subduction-related magma source affected by the metasomatism of sediments or liquids derived from the subducted plate [71, 73].

In the Ce/Pb versus Ce diagram (Figure 12a), samples of the investigated volcanic rocks are located in the arc volcanics area. The low Ce / Pb ratios (0.9 to 9.5) observed in the samples differ from ocean basalts (20 to 30) [65], indicating that the studied volcanic rocks did not derive from the asthenospheric mantle source. Nb / La ratios are useful in determining the partial melting and source composition in volcanic rocks [74]. High Nb / La ratios (> 1) indicate an asthenospheric mantle source like ocean island basalt (OIB), low ratios (<0.5) indicate a lithospheric mantle source [75]. The Nb/La ratios of the studied volcanic rocks are between 0.28 and 0.48 (Table 1), indicating the spinel lherzolitic lithospheric mantle source (Figure 12b). The studied volcanic rocks are located in or near the arc volcanics area on the Figure 12c. Volcanics La / Nb (2.1 to 3.6) and Ba / Nb (24 to 142) ratios indicate the source associated with subduction zone enrichment. During the subduction, LILE and LREE elements are transported upwards by slab-derived fluids [71, 76]. Therefore, the significant LILE and LREE enrichments observed in the studied volcanics indicate an enriched mantle resource compared to the depleted mantle resource [77, 78]. The Th / Y versus Nb / Y diagram (Figure 12d) proposed by [73] is used to separate melting enrichment products and subduction enrichment volcanic rocks. Also, Th/Y and Nb/Y ratios can be used to separate crustal contamination and homogenization in magma source. The studied volcanic rocks trend parallel to the OIB and MORB line (Figure 112d), but they have higher Th/Y ratios compared to them. Therefore, it indicates that the mantle source undergoes metasomatism by subduction zone fluids. This trend points to the main magma derived from the source enriched (metasomatism) of fluids derived through previous (pre-Eocene) subduction processes.

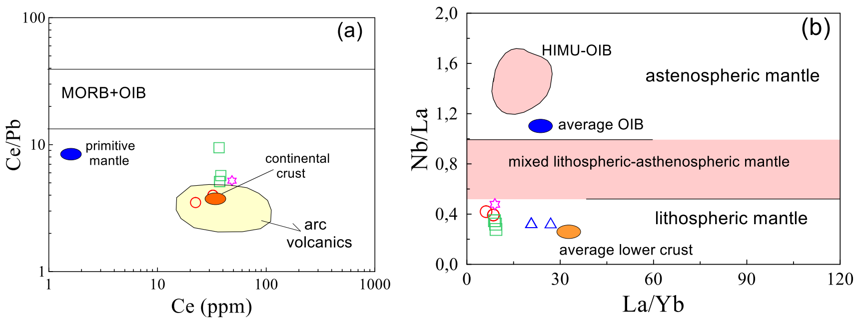

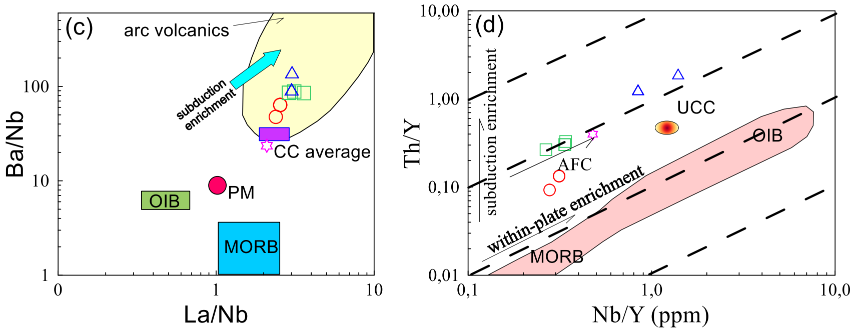

Figure 12. Demirören volcanics' a) Ce/Pb versus Ce diagram, b)) La/Yb versus Nb/La diagram, c) Ba/Nb versus La/Nb diagram [74], d) Th/Y versus Nb/Y diagram [73]. For reference values in diagrams, see Figure 9 caption in [27].

The major and trace element characteristics of the studied Eocene Demirören volcanics are similar to the other Eocene aged volcanic rocks in the Eastern Pontides, and indicate that the main magma that constitutes the studied volcanics may have originated from the sub-continental lithospheric mantle source affected by the metasomatism of fluids derived from subduction related events pre-Eocene time.

7. Conclusions

Basaltic andesite, andesite, dacite and rhyolite type rocks that make up the studied Demirören volcanics generally show microlithic, microlithic porphyritic, porphyritic, hyalo-porphyritic and glomerophyric textures, and the main minerals are plagioclase, alkaline feldspar, quartz, hornblende, augite and biotite. Good positive and negative relationships observed in the Harker diagrams show that fractional crystallization is effective in the development of rocks and clinopyroxene + plagioclase ± hornblende ± Fe-Ti oxide fractionation plays an important role. The distribution of trace elements of the volcanites normalized to the primitive mantle shows enrichment in large ion lithophile elements (LILEs) and light rare earth elements (LREEs), while depleting in high field-strength elements (HFSE). Rare earth element distributions are concave-shaped with low-medium enrichment (La_N/Lu_N = 3.52 to 15.85). Considering the mineralogical, petrographic and geochemical properties of the Eocene volcanics of the Demirören region, it was concluded that the origin magma of the volcanics was probably formed by the partial melting of a sub-continental lithospheric mantle source metasomatized by previous subduction fluids, and then it was exposed to magmatic events such as fractionation ± assimilation.

Acknowledgment

This study was supported by the Coordination Unit of Scientific Research Projects of Gümüşhane University (GÜBAP, Grant Number: 13.F5114.02.08). We would like to thank the editor and reviewer(s) for their contribution during the review and evaluation phase of the article..

References

[1] Vural A. Evaluation of soil geochemistry data of Canca Area (Gümüşhane, Turkey) by means of Inverse Distance Weighting (IDW) and Kriging methods-preliminary findings. Bulletin of The Mineral Research and Exploration 2019; 158:10–20.

[2] Vural A, Ersen F. Geology, mineralogy and geochemistry of manganese mineralization in Gumushane, Turkey. Journal of Engineering Research and Applied Science 2019; 8:1051–1059.

[3] Vural A. Contamination assessment of heavy metals associated with an alteration area: Demirören Gumushane, NE Turkey. Journal of the Geological Society of India 2015; 86:215–222.

[4] Vural A. K-Ar dating for determining the age of mineralization as alteration product: A case study of antimony mineralization vein type in granitic rocks of Gümüşhane area, Turkey. Acta Physica Polonica A 2017; 132:792–795.

[5] Vural A, Erdoğan M. Eski Gümüşhane

Kırkpavli Alterasyon Sahasında Toprak Jeokimyası. Gümüşhane Üniversitesi Fen Bilimleri Enstitüsü Dergisi 2014; 4:1–15.
[6] Vural A, Şahin E. Gümüşhane Şehir Merkezinden Geçen Karayolunda Ağır Metal Kirliliğine Ait İlk Bulgular. Gümüşhane Üniversitesi, Fen Bilimleri Enstitüsü Dergisi 2012; 2:21–35.
[7] Vural A, Çiçek B. Cevherleşme Sahasında Gelişmiş Topraklardaki Ağır Metal Kirliliği. Düzce Üniversitesi Bilim ve Teknoloji Dergisi 2020; 8:1533–1547.
[8] Kaygusuz A, Arslan M, Sipahi F, Temizel İ. U-Pb zircon chronology and petrogenesis of Carboniferous plutons in the northern part of the Eastern Pontides, NE Turkey: Constraints for Paleozoic magmatism and geodynamic evolution. Gondwana Research 2016; 39:327–346.
[9] Kaygusuz A, Arslan M, Temizel İ, CemYücel, Aydınçakır E. U–Pb zircon ages and petrogenesis of the Late Cretaceous I-type granitoids in arc setting, Eastern Pontides, NE Turkey. Journal of African Earth Sciences 2021; 174:104040.
[10] Arslan M, Temizel I, Abdioğlu E, Kolayli H, Yücel C, Boztuğ D, Şen C. 40Ar-39Ar dating, whole-rock and Sr-Nd-Pb isotope geochemistry of post-collisional Eocene volcanic rocks in the southern part of the Eastern Pontides (NE Turkey): Implications for magma evolution in extension-induced origin. Contributions to Mineralogy and Petrology 2013; 166:113–142.
[11] Aslan Z, Arslan M, Temizel I, Kaygusuz A. K-Ar dating, whole-rock and Sr-Nd isotope geochemistry of calc-alkaline volcanic rocks around the Gümüşhane area: Implications for post-collisional volcanism in the Eastern Pontides, Northeast Turkey. Mineralogy and Petrology 2014; 108:245–267.
[12] Kaygusuz A, Şahin K. Petrographical, geochemical and petrological characteristics of Eocene volcanic rocks in the Mescitli area , Eastern Pontides (NE Turkey). Journal of Engineering Research and Applied Science 2016; 5:473–486.
[13] Sipahi F, Akpınar İ, Saydam Eker Ç, Kaygusuz A, Vural A, Yılmaz M. Formation of the Eğrikar (Gümüşhane) Fe–Cu skarn type mineralization in NE Turkey: U–Pb zircon age, lithogeochemistry, mineral chemistry, fluid inclusion, and O-H-C-S isotopic compositions. Journal of Geochemical Exploration 2017; 182:32–52.
[14] Sipahi F, Kaygusuz A, Saydam Eker, Vural A, Akpınar. Late Cretaceous arc igneous activity: the Eğrikar Monzogranite example. International Geology Review 2018; 60:382–400.
[15] Temizel İ, Arslan M, Yücel C, Abdioğlu Yazar E, Kaygusuz A, Aslan Z. U-Pb geochronology, bulk-rock geochemistry and petrology of Late Cretaceous syenitic plutons in the Gölköy (Ordu) area (NE Turkey): Implications for magma generation in a continental arc extension triggered by slab roll-back. Journal of Asian Earth Sciences 2019; 171:305–320.
[16] Temizel İ, Arslan M, Yücel C, Abdioğlu Yazar E, Kaygusuz A, Aslan Z. Eocene tonalite–granodiorite from the Havza (Samsun) area, northern Turkey: adakite-like melts of lithospheric mantle and crust generated in a post-collisional setting. International Geology Review 2020.
[17] Vural A. Demirören/Gümüşhane-Türkiye Kuvars Porfiri Kayacı ve İlişkili Skarn-Metasomatizmanın Jeokimyasal Özellikleri (Geochemical Properties of Demirören/Gümüşhane Quartz Porphyry Rock and Related Skarn- Metasomatism). Euroasia Journal of Mathematics, Engineering, Natural & Medical Sciences 2020; 7:97–121.
[18] Vural A, Kaygusuz A. Geochronology, petrogenesis and tectonic importance of Eocene I-type magmatism in the Eastern Pontides, NE Turkey. Arabian Journal of Geosciences 2021; 14:467.
[19] Çamur MZ, Güven İH, Er M. Geochemical characteristics of the eastern Pontide volcanics: an example of multiple volcanic cycles in arc evolution. Turkish Journal of Earth Sciences 1996:123–144.
[20] Arslan M, Tüysüz N, Korkmaz S, Kurt H. Geochemistry and petrogenesis of the eastern Pontide volcanic rocks, Northeast Turkey. Chemie Der Erde Geochemistry 1997; 57:157–187.
[21] Özsayar T, Pelin S, Gedikoğlu A. Doğu Pontidlerde Kretase. KTÜ Yer Bilimleri Dergisi 1981; 1:65–114.
[22] Karslı O, Chen B, Aydin F, Şen C. Geochemical and Sr-Nd-Pb isotopic compositions of the Eocene Dölek and Sariçiçek Plutons, Eastern Turkey: Implications for magma interaction in the genesis of high-K calc-alkaline granitoids in a post-collision extensional setting. Lithos 2007; 98:67–96.
[23] Kaygusuz A, Öztürk M. Geochronology, geochemistry, and petrogenesis of the Eocene Bayburt intrusions, Eastern Pontide, NE

Turkey: implications for lithospheric mantle and lower crustal sources in the high-K calc-alkaline magmatism. Journal of Asian Earth Sciences 2015; 108:97–116.
[24] Eyüboğlu Y, Dudas FO, Thorkelson D, Zhu DC, Liu Z, Chatterjee N, Yi K, Santosh M. Eocene granitoids of northern Turkey: Polybaric magmatism in an evolving arc–slab window system. Gondwana Research 2017; 50:311–345.
[25] Özdamar Ş, Roden MF, Billor MZ. Petrology of the shoshonitic Çambaşı pluton in NE Turkey and implications for the closure of the Neo-Tethys Ocean: insights from geochemistry, geochronology and SrNd isotopes. Lithos 2017; 284–285:477–492.
[26] Kaygusuz A, Yücel C, Arslan M, Temizel İ, Yi K, Jeong Y-J, Siebel W, Sipahi F. Eocene I-type magmatism in the Eastern Pontides, NE Turkey: Insights into magma genesis and magma-tectonic evolution from whole-rock geochemistry, geochronology and isotope systematics. International Geology Review 2020; 62 (11): 1406–1432.
[27] Kaygusuz A, Arslan A, Siebel W, Şen C. Geochemical and Sr-Nd Isotopic Characteristics of Post-Collisional Calc-Alkaline Volcanics in the Eastern Pontides (NE Turkey). Turkish Journal of Earth Sciences 2011; 20:137–159.
[28] [28] Aydınçakır E. The Petrogenesis of Early-Eocene non-adakitic volcanism in NE Turkey. Lithos 2014; 208:361–377.
[29] Özdamar Ş. Geochemistry and geochronology of late Mesozoic volcanic rocks in the northern part of the Eastern Pontide Orogenic Belt (NE Turkey): Implications for the closure of the Neo-Tethys Ocean. Lithos 2016; 248–252:240–256.
[30] Yücel C, Arslan M, Temizel İ, Abdioğlu Yazar E, Ruffet G. Evolution of K-rich magmas derived from a net veined lithospheric mantle in an ongoing extensional setting: Geochronology and geochemistry of Eocene and Miocene volcanic rocks from Eastern Pontides (Turkey). Gondwana Research 2017; 45:65–86.
[31] Temizel I, Arslan M, Ruffet G, Peucat JJ. Petrochemistry, geochronology and Sr-Nd isotopic systematics of the Tertiary collisional and post-collisional volcanic rocks from the Ulubey (Ordu) area, eastern Pontide, NE Turkey: Implications for extension-related origin and mantle source characteristics. Lithos 2012; 128–131:126–147.
[32] Vural A, Sipahi F. Demirören (Gümüşhane) Fe-skarn yatağının Jeolojik, Jeokimyasal ve kayaç kimyası, köken özellikleri açısından incelenmesi. GÜ Araştırma Fonu (GÜ BAP) 2016.
[33] Topuz G, Altherr R, Kalt A, Satir M, Werner O, Schwarz WH. Aluminous granulites from the Pulur complex, NE Turkey: A case of partial melting, efficient melt extraction and crystallisation. Lithos 2004; 72:183–207.
[34] Topuz G, Altherr R, Siebel W, Schwarz WH, Zack T, Hasözbek A, Barth M, Satır M, Şen C. Carboniferous high-potassium I-type granitoid magmatism in the Eastern Pontides: The Gümüşhane pluton (NE Turkey). Lithos 2010; 116:92–110.
[35] Kaygusuz A, Arslan M, Siebel W, Sipahi F, Ilbeyli N. Geochronological evidence and tectonic significance of Carboniferous magmatism in the southwest Trabzon area, eastern Pontides, Turkey. International Geology Review 2012; 54:1776–1800.
[36] Vural A, Kaygusuz A. Petrology of the Paleozoic Plutons in Eastern Pontides: Artabel Pluton (Gümüşhane, NE Turkey). Journal of Engineering Research and Applied Science 2019; 8:1216–1228.
[37] Kaygusuz A. Geochronological age relationships of Carboniferous Plutons in the Eastern Pontides (NE Turkey). Journal of Engineering Research and Applied Science 2020; 9:1299–1307.
[38] Dokuz A, Karsli O, Chen B, Uysal I. Sources and petrogenesis of Jurassic granitoids in the Yusufeli area, Northeastern Turkey: Implications for pre- and post-collisional lithospheric thinning of the eastern Pontides. Tectonophysics 2010; 480:259–279.
[39] Eker CS, Sipahi F, Kaygusuz A. Trace and rare earth elements as indicators of provenance and depositional environments of Lias cherts in Gumushane, NE Turkey. Chemie Der Erde - Geochemistry 2012; 72:167–177.
[40] Pelin S. Geological study of the area southeast of Alucra (Giresun) with special reference to its petroleum potential. Trabzon, Türkiye: Karadeniz Teknik Üniversitesi Yayın No. 87; 1977.
[41] Alan İ, Balcı V, Keskin H, Altun İ, Böke N, Demirbağ H, Arman S, Elibol H, Soyakıl M, Kop A, Hanilçi N. Tectonostratigraphic characteristics of the area between Çayeli (Rize) and İspir (Erzurum). Bulletin of Mineral Research and Exploration 2019; 158:1–29.
[42] Aydin F, Dokuz A, Kandemir R, Karsli O.

Temporal, geochemical and geodynamic evolution of the Late Cretaceous subduction zone volcanism in the eastern Sakarya Zone, NE Turkey : implications for mantle-crust interaction in an arc setting. Journal of Asian Earth Sciences 2020; 192: 104217.
[43] Aydınçakır E. Subduction-related Late Cretaceous high-K volcanism in the Central Pontides orogenic belt: Constraints on geodynamic implications. Geodinamica Acta 2016; 28:379–411.
[44] Kaygusuz A, Siebel W, Şen C, Satir M. Petrochemistry and petrology of I-type granitoids in an arc setting: The composite Torul pluton, Eastern Pontides, NE Turkey. International Journal of Earth Sciences 2008; 97:739–764.
[45] Topuz G, Okay AI, Altherr R, Schwarz WH, Siebel W, Zack T, Satir M, Sen C. Post-collisional adakite-like magmatism in the Agvanis Massif and implications for the evolution of the Eocene magmatism in the Eastern Pontides (NE Turkey). Lithos 2011; 125:131–150.
[46] Eyuboglu Y, Dudas FO, Santosh M, Yi K, Kwon S, Akaryali E. Petrogenesis and U-Pb zircon chronology of adakitic porphyries within the Kop ultramafic massif (Eastern Pontides Orogenic Belt, NE Turkey). Gondwana Research 2013; 24:742–766.
[47] Tokel S. Doğu Karadeniz bölgesinde Eosen yaşlı kalkalkalen andezitler ve jeotektonizma. Türkiye Jeoloji Kurultayı Büllteni 1977; 20:49–54.
[48] Kaygusuz A, Merdan-Tutar Z, Yucel C. Mineral chemistry, crystallization conditions and petrography of Cenozoic volcanic rocks in the Bahçecik (Torul/Gumushane) area, Eastern Pontides (NE Turkey). Journal of Engineering Research and Applied Science 2017; 6:641–651.
[49] Kaygusuz A, Gucer MA, Yucel C, Aydincakir E, Sipahi F. Petrography and crystallization conditions of Middle Eocene volcanic rocks in the Aydıntepe -Yazyurdu (Bayburt) area, Eastern Pontides (NE Turkey). Journal of Engineering Research and Applied Science 2019; 8:1205–1215.
[50] Kaygusuz A, Selvi D. Crystallization conditions and petrography of eocene volcanic rocks in the Gümüşdamla-Erikdibi area (Bayburt, NE Turkey). Journal of Engineering Research and Applied Science 2020; 9:1529–1537.
[51] Temizel İ, Abdioğlu Yazar E, Arslan M, Kaygusuz A, Aslan Z. Mineral chemistry, whole-rock geochemistry and petrology of Eocene I-type shoshonitic plutons in the Gölköy area (Ordu, NE Turkey). Bulletin of the Mineral Research and Exploration 2018; 157:121–152.
[52] Kaygusuz A, Yücel C, Arslan M, Sipahi F, Temizel İ, Çakmak G, Güloğlu ZS. Petrography, mineral chemistry and crystallization conditions of Cenozoic plutonic rocks located to the north of Bayburt (Eastern Pontides, Turkey). Bulletin of the Mineral Research and Exploration 2018; 157:75–102.
[53] Aydin F, Karslı O, Chen B. Petrogenesis of the Neogene alkaline volcanics with implications for post-collisional lithospheric thinning of the Eastern Pontides, NE Turkey. Lithos 2008; 104:249–266.
[54] Yücel C. Geochronology, geochemistry, and petrology of adakitic Pliocene–Quaternary volcanism in the Şebinkarahisar (Giresun) area, NE Turkey. International Geology Review 2019; 61:754–777.
[55] Kaygusuz A. K/Ar ages and geochemistry of the post-collisional volcanic rocks in the Ilica (Erzurum) area, eastern Turkey. Neues Jahrbuch Fur Mineralogie-Abhandlungen 2009; 186:21–36.
[56] Kaygusuz A, Aslan Z, Aydınçakır E, Yücel C, Gücer MA, Şen C. Geochemical and Sr-Nd-Pb isotope characteristics of the Miocene to Pliocene volcanic rocks from the Kandilli (Erzurum) area, Eastern Anatolia (Turkey): Implications for magma evolution in extension-related origin. Lithos 2018; 296–299:332–351.
[57] Vural A. Zenginleştirilmiş Jeoturizm Güzergahlarına Dair Farkındalık Oluşturulması : Eski Gümüşhane - Dörtkonak Güzergahı[Creation of Awareness of Enhanced Geotourism Routes: Old Gümüşhane-Dörtkonak Route]. Gümüşhane Üniversitesi Sosyal Bilimler Enstitüsü Elektronik Dergisi 2019; 10:250–274.
[58] Le Maitre RW, Bateman P, Dudek A, Keller J, Lameyre J, Le Bas MJ, Sabine PA, Schmid R, Sorensen H, Streckeisen A, Woolley AR, Zanettin B. A Classification of Igneous Rocks and Glossary of Terms: Recommendations of the International Union of Geological Sciences Subcommission on the Systematics of Igneous rocks. Blackwell Scientific Publications, Oxford, U.K.; 1989.
[59] Winchester JA, Floyd PA. Geochemical discrimination of different magma series and their differentiation products using immobile

elements. Chemical Geology 1977; 20:325–343.
[60] Irvine TN, Baragar WRA. A guide to the chemical classification of the common volcanic rocks. Canadian Journal of Earth Sciences 1971; 8:523–548.
[61] Peccerillo A, Taylor SR. Geochemistry of eocene calc-alkaline volcanic rocks from the Kastamonu area, Northern Turkey. Contributions to Mineralogy and Petrology 1976; 58:63–81.
[62] Sun SS, McDonough WF. Chemical and isotopic systematics of oceanic basalts: Implications for mantle composition and processes. Geological Society Special Publication 1989; 42:313–345.
[63] Pearce JA, Cann JR. Tectonic setting of basic volcanic rocks determined using trace element analyses. Earth and Planetary Science Letters 1973; 19:290–300.
[64] Taylor SR, McLennan SM. The Continental Crust; its Composition and Evolution Geoscience Text. Blackwell Scientific Publications, Oxford, U.K.; 1985.
[65] Hoffmann AW. Chemical differentiation of the Earth. The relationship between mantle, continental crust and oceanic crust. Earth and Planetary Science Letters 1988; 90:297–314.
[66] Schmidberger S, Hegner E. Geochemistry and isotope systematics of calc-alkaline volcanic rocks from the Saar-Nahe basin (SW Germany). Implications for Late Hercynian orogenic development. Contributions to Mineralogy and Petrology 1999; 135:373–385.
[67] Drummond MS, Defant M. J. A model for trondhjemite-tonalite-dacite genesis and crustal growth via slab melting: Archean to modern comparisons. Journal of Geophysical Research 1990; 95:21503–21521.
[68] Lambert RJ, Holland JG. Yttrium geochemistry applied to petrogenesis utilizing calcium-yttrium relationships in minerals and rocks. Geochimica et Cosmochimica Acta 1974; 38:1393–1414.
[69] Pearce JA, Bender JF, De Long SE, Kidd WSF, Low PJ, Güner Y, Saroglu F, Yilmaz Y, Moorbath S, Mitchell JG. Genesis of collision volcanism in Eastern Anatolia, Turkey. Journal of Volcanology and Geothermal Research 1990; 44:189–229.
[70] Sun SS, McDonough WF. Chemical and Isotope Systematics of Oceanic Basalts; Implication for Mantle Compositionsand Processes. In: Saunders AD, Nory MJ (eds.), Magmatismin the Ocean Basins. Geological Society of London, Special Publication, 42; 1989:313–345.
[71] Elburg MA, Bergen MV, Hoogewerff J, Foden J, Vroon P, Zulkarnain I, Nasution A. Geochemical trends across an arc-continent collision zone: magma sources and slab-wedge transfer processes below the Pantar Strait volcanoes, Indonesia. Geochimica et Cosmochimica Acta 2002; 66:2771–2789.
[72] McDermott F, Delfin FG, Defant MJ, Turner S, Maury R. The petrogenesis of magmas from Mt. Bulusan and Mayon in the Bicol arc, the Philippines. Contributions to Mineralogy and Petrology 2005; 150:652–670.
[73] Pearce JA. Role of the sub-continental lithosphere in magma genesis at active continental margins. Continental Basalts and Mantle Xenoliths 1983:230–249.
[74] Jahn BM, Wu FY, Lo CH. Crust-mantle interaction induced by deep subduction of the continental crust: geochemical and Sr-Nd isotopic evidence from post-collisional mafic-ultramafic intrusions of the northern Dabie Complex, Central China. Chemical Geology 1999; 157:119–146.
[75] Smith EI, Sanchez A, Walker JD, Wang K. Geochemistry of mafic magmas in the Hurricane Volcanic field, Utah: implications for small- and large-scale chemical variability of the lithospheric mantle. Journal of Geology 1999; 107:433–448.
[76] Churikova T, Dorendorf F, Worner G. Sources and fluids in the mantle wedge below Kamchatka, Evidence from across-arc geochemical variation. Journal of Petrology 2001; 42:1567–1593.
[77] Condie KC, Frey BA, Kerrich R. The 1.75-Ga Iron King Volcanics in westcentral Arizona: a remnant of an accreted oceanic plateau derived from a mantle plume with a deep depleted component. Lithos 2002; 64:49–62.
[78] Zhao D, Lei J, Inoue T, Yamada A, Gao S. Deep structure and origin of the Baikal rift zone. Earth and Planetary Science Letters 2006; 243:681–691.
..